

Supplementary Information

Bright and Stable Gold Nanocluster Assemblies by Silica/Zirconia Double-Shell Encapsulation

Shaochen Zhou^a, Yanyan Duan^b, Kai Liu^a, Robin H. A. Ras^{*, a, c}

a. Department of Applied Physics, School of Science, Aalto University, FI-00076 Espoo, Finland.

b. IMDEA Materials Institute, Calle Eric Kandel 2, Getafe 28906, Spain.

c. Department of Bioproducts and Biosystems, School of Chemical Engineering, Aalto University, FI-00076 Espoo, Finland.

* Corresponding author, E-mail: robin.ras@aalto.fi

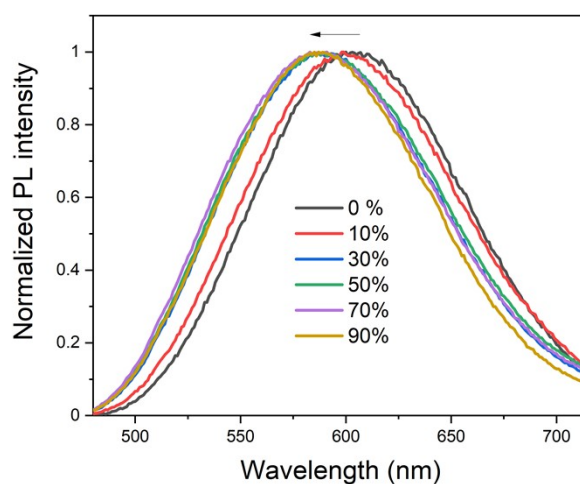


Figure S1. Normalized PL emission spectra of GNC water-ethanol mixture with the volume fraction of ethanol. The emission band keeps blue shifting when the volume fraction of ethanol increases.

Table S1. Absolute photoluminescence quantum yields (PLQYs) of GNCs, GNCA/SiO₂ NPs, and GNCA/SiO₂/ZrO₂ NPs.

Sample	PLQY (%)
GNCs in water	4.76
GNCA/SiO ₂ NPs in ethanol	48.96
GNCA/SiO ₂ /ZrO ₂ NPs in ethanol	54.79

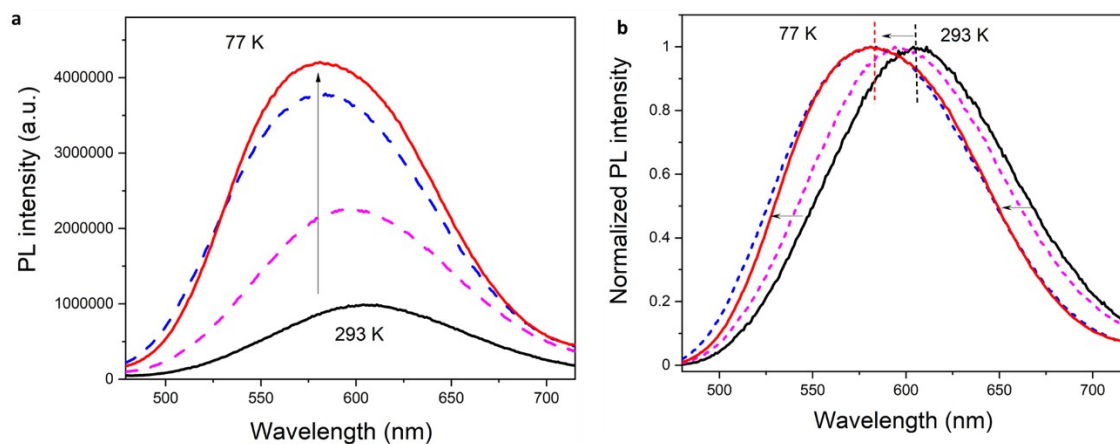


Figure S2. The absolute (a) and normalized (b) PL spectra of GNC aqueous solution at different temperatures. The emission band gradually blue-shifts from 603 nm to 589 nm with a great increase in the emission intensity when the temperature decreases.

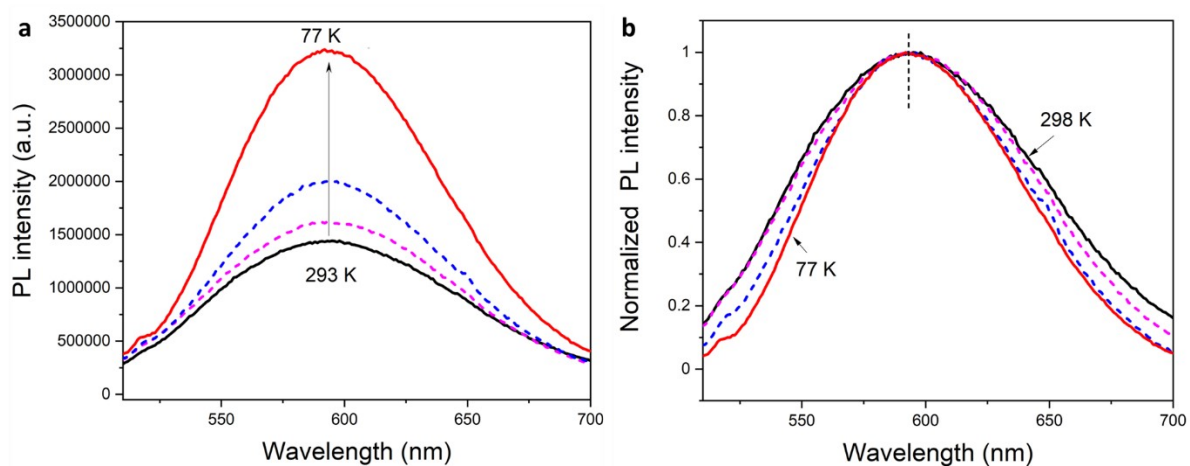


Figure S3. The absolute (a) and normalized (b) PL spectra of GNCA/SiO₂/ZrO₂ NPs at different temperatures. The emission intensity increases with the decreasing temperature. That is because all the thermal motions are further inhibited when the temperature drops, which enhances the emission.

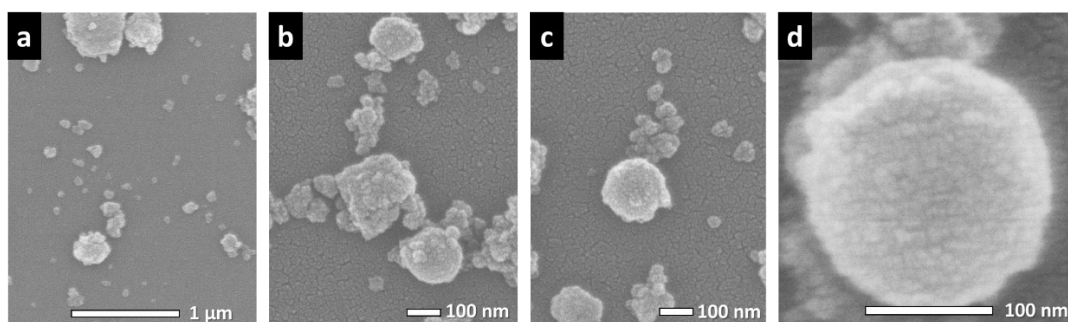


Figure S4. SEM images of GNCA/SiO₂/ZrO₂ NPs.

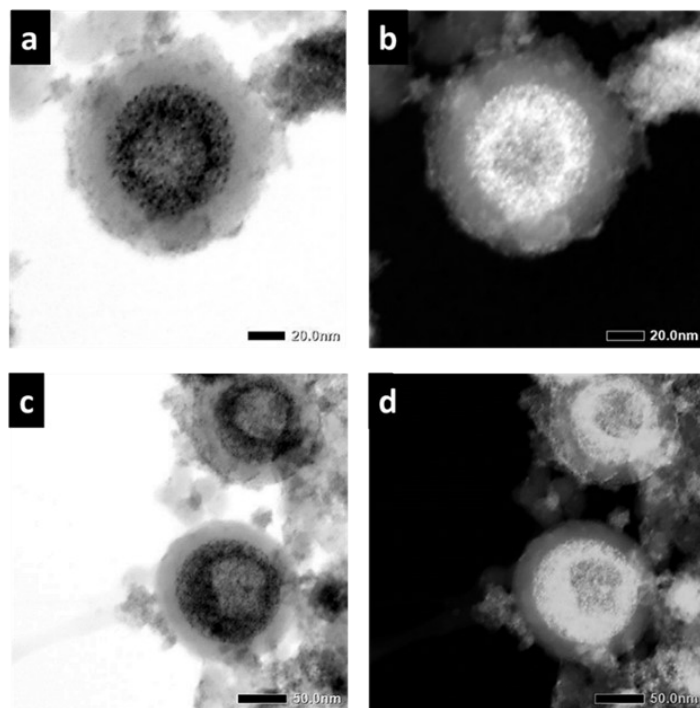


Figure S5. STEM images of GNCA/SiO₂/ZrO₂ NPs in both bright and dark field mode. Spherical assemblies of GNCs are well encapsulated in the shell.

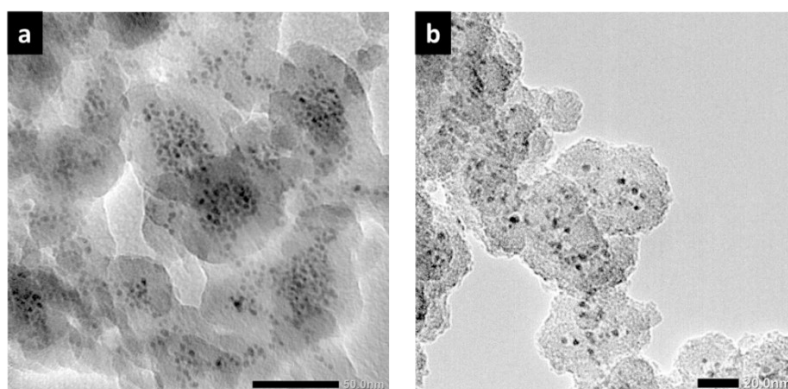


Figure S6. TEM images of GNCA/SiO₂ NPs that are synthesized with insufficient PVP (5 mg/mL).

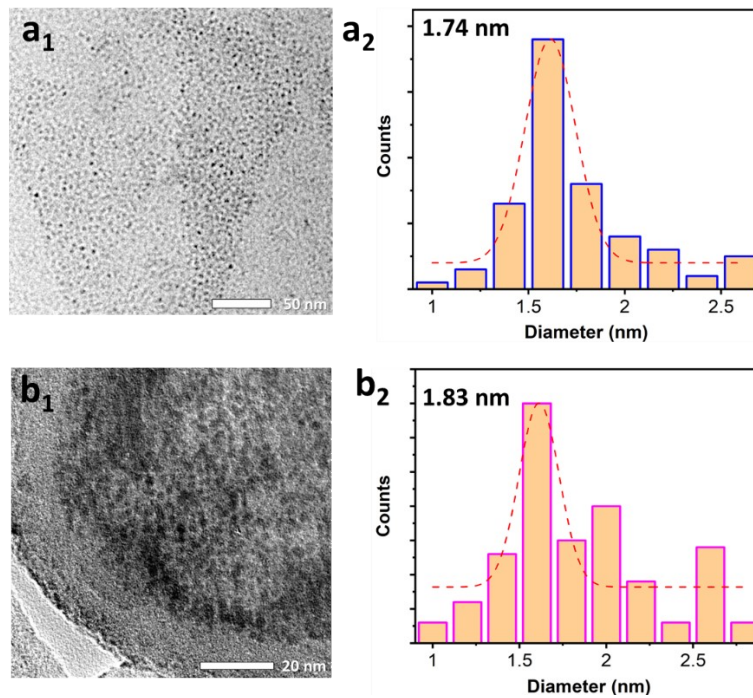


Figure S7. TEM images and size distributions of GNCs (a₁, a₂) and GNCA/SiO₂/ZrO₂ NPs (b₁, b₂). The average diameters of GNCs before and after encapsulation in the oxide matrix are measured to be ~1.7 nm, ~1.8 nm, respectively.

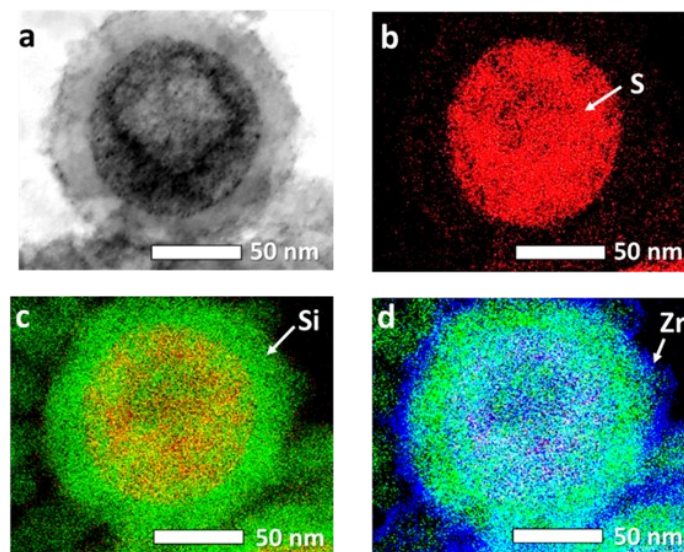


Figure S8. X-ray mapping results. (a) STEM image of a GNCA/SiO₂/ZrO₂ particle. (b) Distribution of S element of the GNCA/SiO₂/ZrO₂ particle. (c) Distribution overlap of S (Red) and Si (green) elements. (d) Distribution overlap of S (Red), Si (green) and Zr (blue) elements.

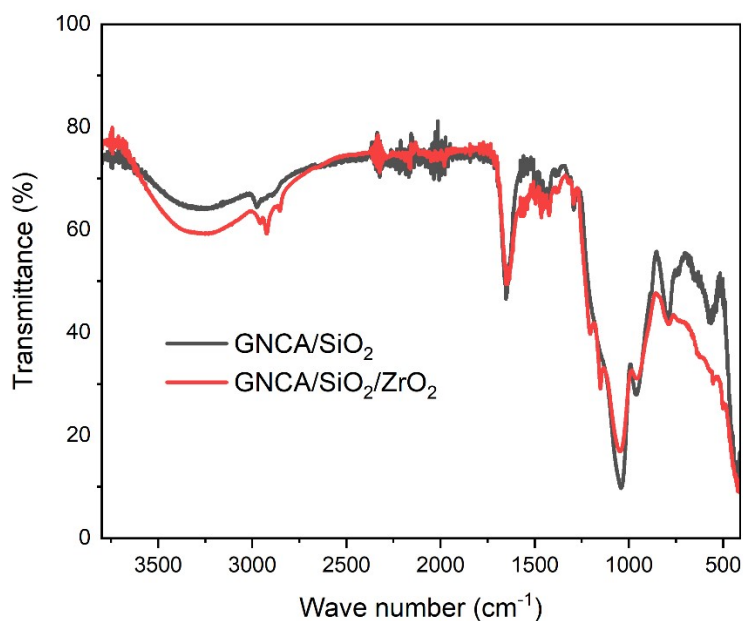


Figure S9. FTIR spectra of GNCA/SiO₂ NPs and GNCA/SiO₂/ZrO₂ NPs. The transmittance of GNCA/SiO₂/ZrO₂ NPs is greater than that of GNCA/SiO₂ NPs in the range of 400~800 cm⁻¹, due to the vibration of Zr-O bonds.

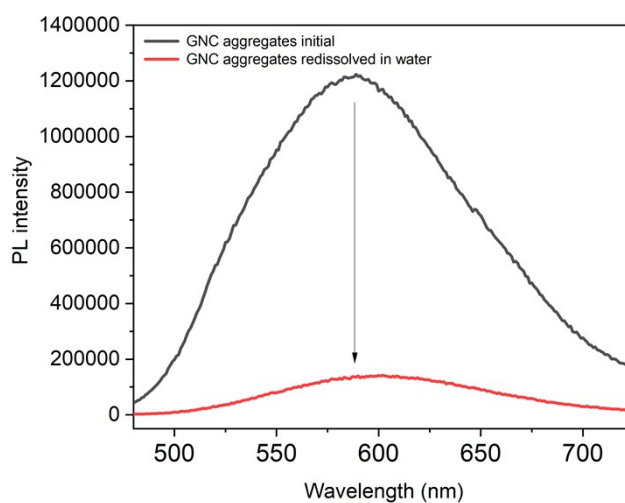


Figure S10. PL emission spectra of bare GNCA aggregates before (black) and after (red) redispersion in water. A conspicuous intensity drop can be observed because bare GNCA aggregates (without stabilization by PVP) are weakly bonded and the hydrophilic GNCA aggregates are extremely prone to separation and dispersion in water.

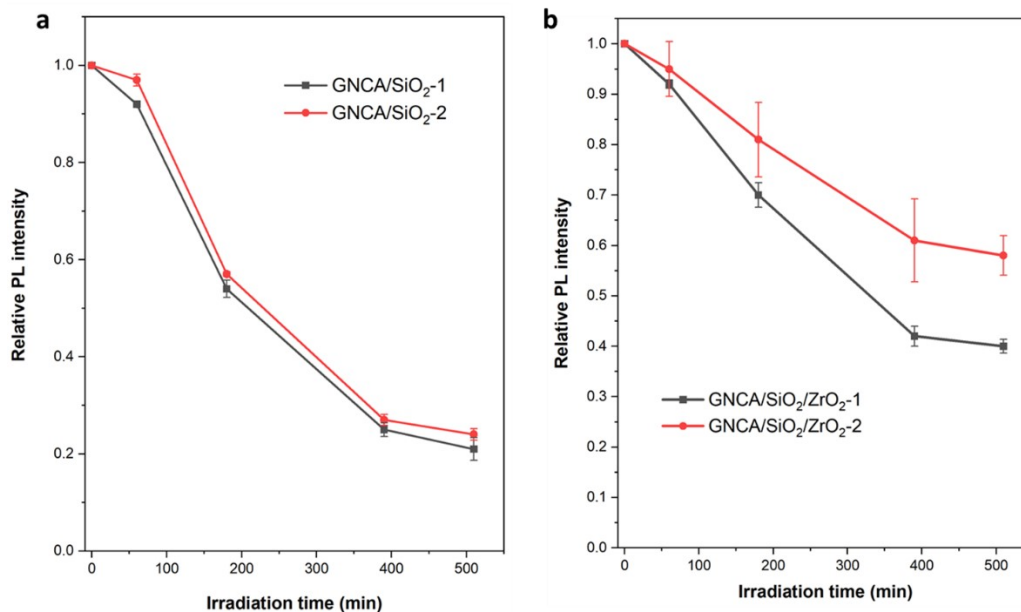


Figure S11. Relative PL intensity evolution of GNCA/SiO₂ NPs and GNCA/SiO₂/ZrO₂ NPs with different shell thicknesses under UV irradiation at 350 nm, 5.96 mw/cm². Amount of silica in GNCA/SiO₂-2 is as ~2 times as that in GNCA/SiO₂-1. Amount of zirconia in GNCA/SiO₂/ZrO₂-2 is as ~2 times as that in GNCA/SiO₂/ZrO₂-1 (amount of silica is the same). More details are shown in Table S2.

Table S2. Molar ratios of Au : Si : Zr in different GNCA/SiO₂ NPs and GNCA/SiO₂/ZrO₂ NPs, and their residual PL intensity with respect to the initial value under UV irradiation for 510 min.

Sample	n (Au) : n(Si) : n(Zr)	Residual relative PL intensity (%)
GNCA/SiO ₂ -1	1:2800:0	21
GNCA/SiO ₂ -2	1:5600:0	24
GNCA/SiO ₂ /ZrO ₂ -1	1:2800:650	40
GNCA/SiO ₂ /ZrO ₂ -2	1:2800:1300	58